**ORIGINAL RESEARCH ARTICLE**

WILEY *Journal of* Cellular Physiology

# Super-resolution structure of DNA significantly differs in buccal cells of controls and Alzheimer's patients

Angeles Garcia[1] | David Huang[2] | Amanda Righolt[2] | Christiaan Righolt[2] |
Maria Carmela Kalaw[2] | Shubha Mathur[2] | Elizabeth McAvoy[1] |
James Anderson[1] | Angela Luedke[1] | Justine Itorralba[1] | Sabine Mai[2]

[1] Department of Medicine (Geriatrics) and Neuroscience Center, Queen's University, SMOL, Kingston, Ontario, Canada

[2] Department of Physiology and Pathophysiology, Manitoba Institute of Cell Biology, University of Manitoba, CancerCare Manitoba, Winnipeg, Manitoba, Canada

**Correspondence**
Sabine Mai, PhD, Department of Physiology and Pathophysiology, Manitoba Institute of Cell Biology, University of Manitoba, CancerCare Manitoba, 675 McDermot Avenue, Winnipeg, R3E 0V9 MB, Canada.
Email: sabine.mai@umanitoba.ca

The advent of super-resolution microscopy allowed for new insights into cellular and physiological processes of normal and diseased cells. In this study, we report for the first time on the super-resolved DNA structure of buccal cells from patients with Alzheimer's disease (AD) versus age- and gender-matched healthy, non-caregiver controls. In this super-resolution study cohort of 74 participants, buccal cells were collected and their spatial DNA organization in the nucleus examined by 3D Structured Illumination Microscopy (3D-SIM). Quantitation of the super-resolution DNA structure revealed that the nuclear super-resolution DNA structure of individuals with AD significantly differs from that of their controls ($p < 0.05$) with an overall increase in the measured DNA-free/poor spaces. This represents a significant increase in the interchromatin compartment. We also find that the DNA structure of AD significantly differs in mild, moderate, and severe disease with respect to the DNA-containing and DNA-free/poor spaces. We conclude that whole genome remodeling is a feature of buccal cells in AD.

**KEYWORDS**
Alzheimer's disease, buccal cells, super-resolution microscopy

## 1 | INTRODUCTION

### 1.1 | Spatial organization of the nucleus

The concept of nuclear architecture linked to proper cellular function is established since the early work of Boveri (1914, 1929).

Sophisticated experimental and analytical tools have become available since then. These technological advances have enabled today's researchers to add detail to Boveri's concept. We have learned that chromosome territories are the structure of chromosomes in interphase nuclei (Cremer & Cremer, 2001; Cremer et al., 2006; Fritz et al., 2016; Sehgal et al., 2016a) and were able to depict all of them together using successive hybridizations (Bolzer et al., 2005). We learned that chromosome positions are conserved during evolution

(Tanabe et al., 2002) and that gene-poor and gene-dense chromosomes have their specific nuclear location in human cells (Tanabe et al., 2002).

Chromosome positioning is not a constant feature of nuclei as positional changes were recorded during keratinocyte differentiation (Sehgal et al., 2016b), during adipocyte differentiation (Charó, Rodríguez Ceschan, Galigniana, Toneatto, & Piwien-Pilipuk, 2016; Kuroda et al., 2004), after PHA-activation of lymphocytes (Ioannou, Kandukuri, Simpson, & Tempest, 2015), and after serum deprivation/ stimulation (Mehta, Amira, Harvey, & Bridger, 2010). It thus appears that the nuclear organization of the genome is directly associated with its cellular function. The first study that was able to directly link chromosome territories and their positions to cellular function was by Solovei et al. (2009). The authors demonstrated that the organization

of chromosome territories differs in the rod nuclei of retinas in diurnal and nocturnal animals: In diurnal animals across the phylogenetic tree, most heterochromatin is observed at the nuclear periphery and euchromatin in the nuclear interior (Solovei et al., 2009). The rod nuclei of nocturnal animals; however, showed an inverted pattern with heterochromatin found in the nuclear center and euchromatin at the nuclear border. The authors concluded that this inverted organization of chromatin in rod cell nuclei acts as collecting lenses in nocturnal animals.

## 1.2 | Super-resolution microscopy

The 2014 Nobel Prize in Chemistry was awarded to Drs. Eric Betzig, William E. Moerner, and Stefan Hell for "the development of super-resolved fluorescence microscopy," a transformative breakthrough that allows imaging of objects far smaller than the Abbe diffraction-limited spatial resolution (200 nm) and enables the study of individual molecules at ≤20 nm. While others have used this new approach to study open questions in immunology (Hu, Cang, & Lillemeier, 2016), cell biology and DNA repair (Lopez Perez et al., 2016), nuclear envelope and nuclear pores (Schermelleh et al., 2008; Xie, Horn, & Wright, 2016), in cells undergoing ischemic stress (Kirmes et al., 2015), and plant biology (Urban, Barclay, Sivaguru, Punyasena, 2016), we were the first to apply this technology to the study of the cancer cell genome (Righolt et al., 2014; Righolt, Knecht, & Mai, 2016; Sathitruangsak et al., 2015). We examined nuclear DNA organization of normal, premalignant, and malignant cells. Nuclei of cancer cells showed more DNA-free and DNA-poor spaces compared to normal cells (Righolt et al., 2014, 2016; Sathitruangsak et al., 2015). We developed a program to quantify the organization of nuclear DNA, using a measurement called granulometry, and applied it to the acquired super resolution images (Righolt et al., 2014, 2016; Sathitruangsak et al., 2015). In these images, the granulometry of the image ("light granulometry") quantifies the DNA structure, and granulometry of the negative ("dark granulometry") quantifies the spaces void of DNA structure (Righolt et al., 2014). An increase in dark granulometry shows that DNA-poor space is increased in frequency, size, or both (Righolt et al., 2014).

## 1.3 | Alzheimer's and nuclear structural markers of Alzheimer's disease

Alzheimer's disease (AD) is an increasing challenge for society. According to the Alzheimer's Society, an estimated 5.4 million Americans of all ages live with AD in 2016. This number includes an estimated 5.2 million people age 65 and older (Alzheimer's Association, 2016; Hebert, Weuve, Scherr, & Evans, 2013), and approximately 200,000 individuals under the age of 65 who have younger-onset AD (Alzheimer's Association, 2016; Hebert et al., 2013). World-wide, nearly 44 million people suffer from AD and related dementias (http://www.alzheimers.net/resources/alzheimers-statistics/). The costs to the health care systems are immense: Currently, the costs amount to $236 billion in the United States. In 2050, it is expected to reach $1 trillion (http://www.alz.org/facts/). No treatment for the disease that slows or reverses it has been identified to date.

In a previous study, we have focused on the spatial organization of telomeres in buccal cells of AD (Mathur et al., 2014). Buccal cells are of neuroectodermal origin and therefore considered a suitable model for studies into changes observed in the brain (Forero et al., 2016; Mathur et al., 2014; Thomas, O'Callaghan, & Fenech, 2008). Our previous study (Mathur et al., 2014) was a blinded study with 41 AD patients and 41 age- and gender-matched caregivers. We measured the 3D nuclear telomere organization using TeloView (Vermolen et al., 2005) and showed that the 3D telomeric organization in buccal cells of the 82 study participants was significantly different in AD and non-AD. Moreover, the 3D telomeric profiles were significantly different between mild, moderate, and severe AD patients. The 3D profiles described alteration in the number of telomeric signals detected, the telomere length measured and the aggregation of telomeric signals (Mathur et al., 2014). A recent meta analysis that focuses on telomere length alone has confirmed our findings of shorter telomeres in AD as a general feature of AD (Forero et al., 2016).

In the current study, we have investigated the nuclear organization of DNA in AD and non-AD using quantitative 3D-SIM super resolution microscopy. Our non-AD control participants were gender- and age-matched non-caregivers as caregivers were shown to exhibit telomere shortening as a result of constant and long-lasting daily stress (Damjanovic et al., 2007; O'Donovan et al., 2012). Our data show for the first time evidence for AD-specific nuclear DNA organization.

**TABLE 1** Demographics and AD scores of 74 study participants

| Population | Test score ranges (MoCA/30:MMSE/30) | Number of subjects | Mean age (years ± SD) | Gender (male/female) |
|---|---|---|---|---|
| Mild AD | >18:≥22 | 19 | 76.4 ± 9.1 | 6/13 |
| Controls, mild AD | N/A | 19 | 75.2 ± 8.6 | 6/13 |
| Moderate AD | ≤18:21–16 | 14 | 77.2 ± 7.9 | 6/8 |
| Controls, moderate AD | N/A | 14 | 76 ± 13.5 | 6/8 |
| Severe AD | ----:<16 | 4 | 85 ± 2.9 | 1/3 |
| Controls, severe AD | N/A | 4 | 81.7 ± 3.5 | 1/3 |

AD, Alzheimer's disease; MoCA, Montreal Cognitive Assessment, MMSE, Mini-Mental State Examination.
All patients were on treatment with cholinesterase inhibitors.

# 2 | MATERIALS AND METHODS

## 2.1 | Study participants

Diagnosis of AD was made at the Queen's Memory Clinic according to the National Institute of Neurological and Communicative Disorders and Stroke, and the Alzheimer's Disease and Related Disorders Association (NINCDS-ADRDA) criteria (Dubois et al., 2007; McKhann et al., 1984). Patients presented as mild, moderate, or severe AD based on their regular clinic visits and their scores on the Montreal Cognitive Assessment (MoCA) and the Mini-Mental State Examination (MMSE) (Table 1) (Folstein, Folstein, & McHugh, 1975; McDowell, Kristjansson, Hill, & Hebert, 1997; Nasreddine et al., 1995). Patients with a MoCA score of >18/30 and/or MMSE score of ≥22/30 were categorized as mild AD. Patients with a MoCA score of ≤18/30 and/or MMSE score between 21/30 and 16/30 were considered to be in the moderate stage of AD, whereas patients with an MMSE score lower than 16/30 were classified as severe AD (Table 1) (Folstein et al., 1975; McDowell et al., 1997; Nasreddine et al., 1995). All AD patients were treated with cholinesterase inhibitors according to the Canadian guidelines for treatment of dementia (Gauthier et al., 2012; Herrmann & Gauthier, 2008). Our study examined buccal cells of 37 patients diagnosed with AD who were compared to 37 gender- and age-matched cognitively normal and healthy controls. We evaluated 19 mild AD patients and their 19 controls, 14 moderate AD patients and their 14 controls, and 4 severe AD patients and their 4 controls. Since the focus of our work was on mild and moderate AD, the numbers of severe AD in this study are very low. Our study was approved by the Queen's University Research Ethics Board and by the University of Manitoba Ethic's Board (HS 16926(H2013:465)), and all 74 participants provided written informed consent.

## 2.2 | Buccal cell collection

Buccal swabs were collected from each study participant and placed onto slides. The cells were verified to be of high quality by the Queen's Memory Clinics' personnel and collaborating physician. Briefly, using Epicentre Catch-A11 sample collection swabs, buccal cells were collected in duplicate from each participant and smeared onto microscope VWR pre-cleaned frosted micro slides immediately afterward. Once slides were air-dried, they were frozen at −20°C until shipped to the University of Manitoba on dry ice.

## 2.3 | Buccal cell staining for 3D-SIM studies

Cells placed on slides were 3D-fixed to preserve their 3D nuclear architecture using 3.7% formaldehyde in 1 × phosphate buffered saline (1 × PBS) for 20 min at room temperature (Solovei et al., 2002). Following three washes in 1 × PBS (5 min each, shaking, at room temperature), the slides were stained with 4′,6-diamidino-2-phenylindole (DAPI) (1 µg/ml) for 3 min and subsequently embedded in a drop of Vectashield (Vector Laboratories, Burlington, ON, Canada). A coverslip specially suited for super-resolution microscopy was added (No. 1 ½, Schott, Mainz, Germany), sealed with nail polish and imaged immediately.

## 2.4 | Super-resolution imaging

3D-SIM images were recorded as described previously (Righolt et al., 2014). Briefly, all images were acquired with a Zeiss ELYRA PS1 (Zeiss, Toronto, Ontario, Canada) equipped with a Plan-Apochromat 63×/1.40 Oil immersion objective using an Andor EM-CCD iXon 885 camera and a 1.6× tube lens. The DAPI channel was obtained with 405 nm laser excitation, 23 µm diffraction grating and filter cube SR Cube 07. The lateral pixel size, $\Delta x$ and $\Delta y$, was 79 nm in the recorded images and 40 nm in the reconstructed image, the step between z-planes, $\Delta z$, was 91 nm. The 3D-SIM images were reconstructed with ZEN 2012 black edition (Carl Zeiss, Jena, Germany) with the standard settings except for the regularization parameter, which was set to $10^{-3}$, and clipping, which was turned off. Clipping the image in the reconstruction stage was not done, because it sets the background to zero (black), hides actual image information and artificially increases the perceived resolution.

## 2.5 | Image processing

The image processing and measurement steps were performed in Matlab (MathWorks, Natick, MA) with the toolbox DIPimage (Luengo Hendriks et al., 1999). A central z-plane was manually selected for processing (Righolt et al., 2014). The nucleus was automatically detected by isodata thresholding (Ridler & Calvard, 1978) the widefield DAPI image and filling the holes in the binary image. The greyscale DAPI images were error-function clipped between the 10th and 90th percentile of the intensity over the detected cell (Verbeek & van Vliet, 1993). The granulometry (3D Signatures Inc., Winnipeg, MB, Canada) of the DNA structure and DNA-free space was measured with a morphological sieve applied to the unclipped images (Luengo Hendriks et al., 2007).

## 2.6 | Nuclear aspect ratio measurements

Nuclear aspect ratios of all 2,220 nuclei were manually measured as shown in Supplemental Fig. 1. Line measurements of the "major" and "minor" lengths were done through each nucleus and the differences between the two calculated.

## 2.7 | Statistical analyses

The coefficient of variation (the standard deviation divided by the mean) and skewness of the intensity histogram over the detected region was computed as well. To assess the significance of the measured difference, we used two-sided, two-sample Kolmogorov–Smirnov (KS) tests. A linear classification line based on the Fisher linear discriminant assuming equal priors was performed for the histogram features using the PRTools toolbox for Matlab (Duin, 2007). The structure of the DNA and DNA-poor space were compared between cases and controls by controlling for both granular size and matching

using a general linear models (GLM). Abnormal/normal cell proportions were analyzed by Mantel–Haenszel stratified analysis. The nuclear aspect ratio data were analyzed using the GLM procedure.

## 3 | RESULTS

### 3.1 | Buccal cell analysis of Alzheimer's disease (AD) and matched controls

We examined buccal cells of 74 study participants to define the DNA super-resolution structure of their nuclei based on 3D Structured Illumination Microscopy (3D-SIM), a super resolution imaging method. Table 1 summarizes the participant information and their respective Alzheimer's Disease (AD) scores (mild, moderate, or severe) based on their regular clinic visits and their scores obtained on the Montreal Cognitive Assessment (MoCA) and the Mini-Mental State Examination (MMSE) tests (Folstein et al., 1975; McDowell et al., 1997; Nasreddine et al., 1995). Scoring of the AD study participants was carried out by a clinician (AG).

### 3.2 | Super-resolution DNA structure of buccal cells of AD and non-AD study participants

Buccal cells of all participants were imaged using 3D-SIM and subjected to granulometry analyses (Righolt et al., 2014). Light granulometry represents DNA structure as detected by 3D-SIM of 4′,6-diamidino-2-phenylindole (DAPI)-stained nuclei. In contrast, dark granulometry refers to spaces void of DAPI signals and thus spaces representing DNA-free/poor spaces detected in nuclei or the interchromatin compartment.

Figure 1 illustrates the DNA structure of representative buccal cell nuclei in AD and non-AD (dark vs. light granulometries). The organization of the DNA differs significantly between normal age- and gender-matched individuals and the AD patients that scored with mild, moderate, or severe disease: Granulometry measurements were carried out (Table 2, Fig. 2). Figure 2 shows representative examples of light and dark granulometries representing the DNA-free spaces for mild, moderate, and severe AD versus non-AD controls, respectively (Fig. 2 Panel A and B). Statistical analyses were performed on 2,220 nuclei from 74 study participants (i.e., on 30 nuclei per person) that had been imaged with 3D-SIM and analyzed by light and dark granulometries (Table 2). For all AD severities combined and compared to the non-AD controls, we found significant alterations in the DNA-poor spaces where dark granulometry increased ($p < 0.0001$). In contrast, the amount of DNA measured (light granulometry) was not significantly different ($p = 0.6859$). These data indicate that, as expected, no DNA is lost or gained between non-AD controls and AD subjects. However, the spatial organization of the DNA in the 3D nucleus is significantly remodeled in AD leaving these nuclei with more DNA-free/poor space and therefore a larger interchromatin compartment.

When individual comparisons were performed, distinctive features for each group became apparent. Buccal cells of mild AD manifest significant organizational differences in both light and dark granulometries ($p < 0.0001$ and $p = 0.0009$, respectively). Buccal cells of moderate AD display light granulometries distinct from those of non-AD ($p < 0.0001$) but not dark granulometries ($p = 0.5704$). Buccal
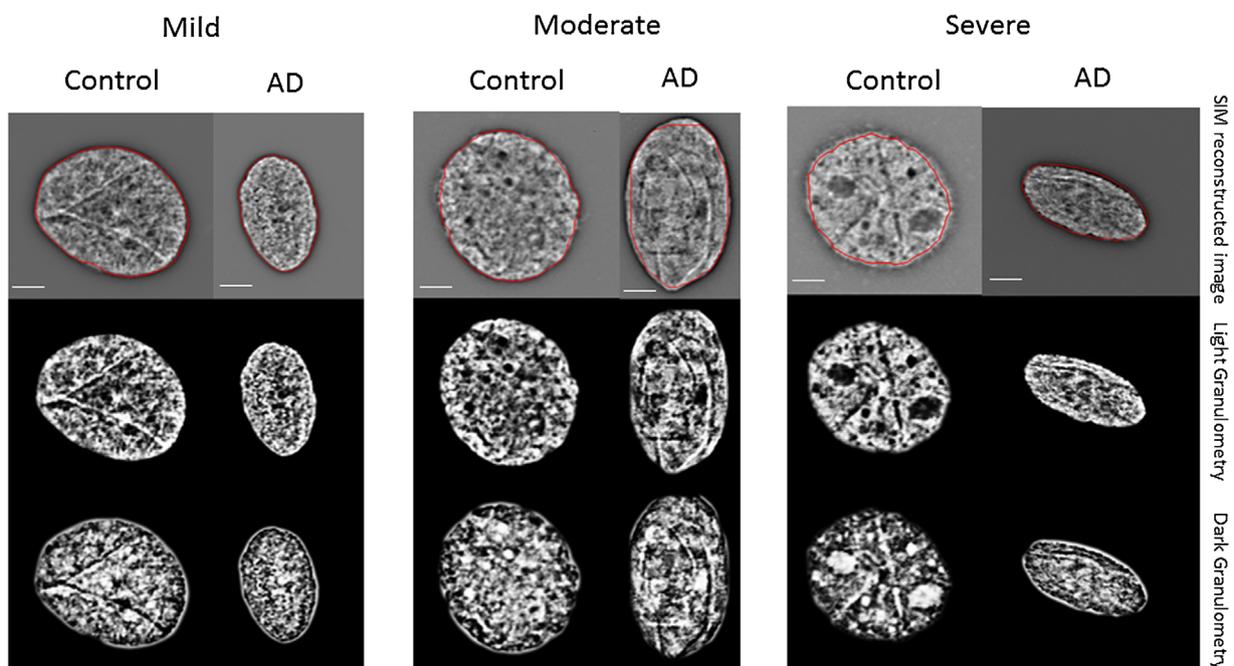


**FIGURE 1** Representative 3D-SIM images of buccal cell nuclei collected from Alzheimer's (AD) and controls and their respective light and dark granulometry images. Buccal cells were collected, placed onto slides and stained as described (Section 2). Buccal cell nuclei from mild, moderate and severe AD were compared to their age- and gender-matched non-AD controls. Top images: reconstructed 3D SIM images, middle images: light granulometry images; bottom images: dark granulometry images. For statistical analyses, see Table 2. Scale bar: 1 μm

**TABLE 2** Light and dark granulometry results of buccal cell nuclear DNA of 74 study participants, imaged by 3D-SIM

|  | Light granulometry | Dark granulometry |
| --- | --- | --- |
| All AD versus control | $p = 0.6859$ | $p < 0.0001$ |
| Mild AD versus control | $p < 0.0001$ | $p = 0.0009$ |
| Moderate AD versus control | $p < 0.0001$ | $p = 0.5704$ |
| Severe AD versus control | $p = 0.1427$ | $p < 0.0001$ |

cells of severe AD exhibit significant differences in dark granulometries ($p < 0.0001$), while light granulometries are similar to those of the controls ($p = 0.1427$). These data indicate dynamic changes to the 3D nuclear organization of DNA during the onset and progression of the disease (Table 2).

## 3.3 | Nuclear aspect ratios of buccal cells from AD and non-AD study participants

While performing the above studies, we noted changes in the nuclear shapes of buccal cells at 3D-SIM resolution. We examined the nuclear dimensions (minor, major, and difference) for the above 2,220 nuclei as a simple evaluation method for nuclear morphology (Section 2 and Supplemental Fig. 1). While it is known that buccal cells have several sub-types (François et al., 2016), we have not selected for any subtype but rather collected data from all types present in a study participants' collected sample. Combining all buccal of all AD groups compared to all buccal cells of the controls yielded significant differences in the nuclear aspect ratios ($p = 0.0296$) (Supplemental Table S 1). This result indicates that the overall shape of the nuclei is more ellipsoid in buccal cells of AD than in non-AD. When this measurement is broken down into the AD subgroups of mild, moderate, and severe, it is not a strong discriminator between the AD subgroups (Supplemental Table S 1).

## 4 | DISCUSSION

The data presented in this study highlight novel features of the nuclear architecture of buccal cells of patients with AD compared to gender- and age-matched controls. Our data demonstrate a significant increase in DNA-free/poor space in AD accompanied by some changes in nuclear morphology.

### 4.1 | 3D nuclear space and genomic remodeling in disease

This work illustrates that the 3D nuclear organization of the genome is changed in patients with AD compared to age- and gender-matched controls. This finding is new for AD, but in agreement with other observations that associate the organization of the nucleus with its overall function in normal and diseased cells. While we do not know what leads to the changes in cells of individuals with AD, we have some knowledge on the genetic, environmental, and molecular mechanisms that alter the 3D nuclear organization in normal cells and in diseased cells (Charó et al., 2016; Gadji et al., 2011; Ioannou et al., 2015; Kuroda et al., 2004; Lajoie et al., 2015; Louis et al., 2005; Matarazzo, Boyle,

D'Esposito, & Bickmore, 2007; Mehta et al., 2010). It is in this general context that Meaburn (2016), in a recent review, poses the question whether the spatial organization of the genome may serve as a potential biomarker of disease. She writes, "Since spatial reorganization of the genome has been identified in multiple human diseases, it is likely that spatial genome positioning patterns as a diagnostic biomarker may be applied to many diseases."

With respect to AD, the super-resolved organization of the genomic DNA structure may be stage-specific as our study indicates. This conclusion complements our previous study that demonstrated the nuclear remodeling of telomeres in the 3D space of AD versus non-AD as a stage-specific event for mild, moderate, and severe AD versus controls (Mathur et al., 2014). In addition to the remodeling, telomeres were also significantly shorter, and this was confirmed in a recent meta-analysis (Forero et al., 2016).

There may be dynamic changes in the organization of the genome structure and its associated function that enable the remodeling of the genome in AD. While not yet reported for AD, other studies have reported that nuclear re-organization occurs and may be linked to neuronal differentiation and disease. In a recent review, Wilczynski (2014) summarized current evidence on large-scale chromatin changes in neuronal differentiation, seizures, disorders of neuronal plasticity, and epilepsy. Furthermore, the role of epigenetics in AD has been studied, and several groups suggest that epigenetic changes play a role in the disease (Klein, Bennett, & De Jager, 2016; for a general review, see Alexander and Lomvardas, 2014). How epigenetic alterations exactly act upon the remodeling of DNA in the 3D space of the genome (and in AD) or how epigenetic changes drive the structural remodeling of the genome is currently unknown and warrants further investigations.

### 4.2 | Super resolution DNA structure

Due to the lack of super resolved data on 3D nuclear DNA and chromosome organization, no exact knowledge about the nuclear organization of the genome existed up to very recently. Pioneering studies into the 3D spatial genome arrangement (Markaki et al., 2010) indicate that nuclei of normal cells show a network of channels and wider lacunas, called the interchromatin compartment (IC). This spatial genomic and DNA-free network is dynamic in nature: Recent work in cells under ischemic stress has shown that the IC can expand upon ischemic stress and revert back to normal conditions (Kirmes et al., 2015; for review, see Cremer et al., 2015). Our recent work on the super resolution DNA structure in Hodgkin's lymphoma and multiple myeloma highlighted the increase in DNA-free/poor space in nuclei of these cancer cells (Righolt et al.,
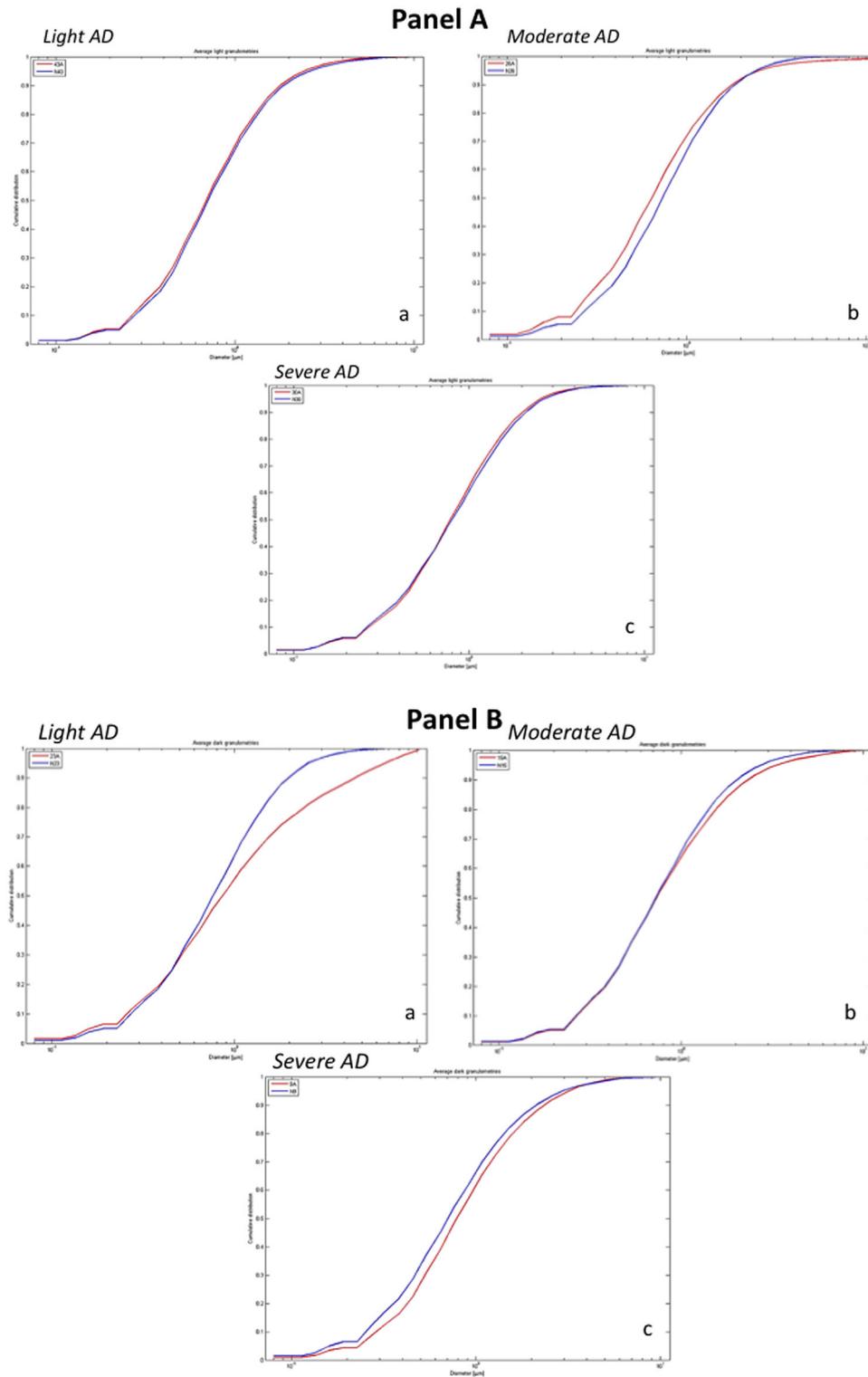
**FIGURE 2** Representative light and dark granulometry measurements for buccal cell nuclei of representative individual cases of mild, moderate, and severe AD and their matched non-AD controls. Cumulative distribution versus diameter (in μm) is given for each graph. Panel A: Light granulometries for mild (a), moderate (b), and severe AD (c) (red lines) with their respective non-AD controls (blue lines). Panel B: dark granulometries for mild (a), moderate (b), and severe AD (c) (red lines) with their respective non-AD controls (blue lines). The $p$-values for the individual representative cases shown in this figure are as follows; Panel A (a): $p = 0.75$, Panel A (b): $p = 8.98906E-12$, Panel A (c): $p = 0.76$, Panel B (a): $p = 3.80385E-17$, Panel B (b): $p = 0.047$, Panel B (c): $p = 7.48055E-05$. For statistical analyses of all AD versus controls in each group, see Table 2

2014, 2016; Sathitruangsak et al., 2015). The data of the current study on the super resolution structure of AD versus non-AD indicate that the IC compartment increases significantly in AD. Together, all available data suggest that the previously discussed models of the interchromatin domain and interchromosomal network arrangement of the genome (reviewed in Branco & Pombo, 2006) can be tentatively answered in favor of the interchromosomal model that assumes spaces in between chromosomes. In contrast, the interchromosomal network model assumes that chromosome territories mix and form contacts with each other in the absence of interchromosomal space. This latter model is not supported by the experimental evidence revealed by super-resolution studies. In fact, all data obtained by super resolution suggest that the IC is a dynamic feature of the genome and its overall plasticity. This holds true for AD as well as shown in the current study. In conclusion, buccal cells of AD patients show a significant increase in interchromosomal space.

## ACKNOWLEDGMENTS

## REFERENCES

Alexander, J. M. & Lomvardas, S. (2014) Nuclear architecture as an epigenetic regulator of neural development and function. *Neuroscience*, 264, 39–50. doi: 10.1016/j.neuroscience.2014.01.044

Alzheimer's Association. (2016). Alzheimer's disease facts and figures. https://www.alz.org/documents_custom/2016-facts-and-figures.pdf.

Bolzer, A., Kreth, G., Solovei, I., Koehler, D., Saracoglu, K., Fauth, C., ... Cremer, T. (2005). Three-dimensional maps of all chromosomes in human male fibroblast nuclei and prometaphase rosettes. *PLoS Biology*, 3, e157.

Boveri, T. (1914). *Zur frage der entstehung maligner tumoren*. Jena: Fischer.

Boveri, T. (1929). *The origin of malignant tumors. Translated by Marcella Boveri*. Baltimore: The Williams & Wilkens Company.

Branco, M. R. & Pombo, A. (2006). Intermingling of chromosome territories in interphase suggests role in translocations and transcription-dependent associations. *PLoS Biology*, 4, e138.

Charó, N. L., Rodríguez Ceschan, M. I., Galigniana, N. M., Toneatto, J., & Piwien-Pilipuk, G. (2016). Organization of nuclear architecture during adipocyte differentiation. *Nucleus*, 7, 249–269. doi: 10.1080/19491034.2016.1197442

Cremer, T. & Cremer, C. (2001). Chromosome territories, nuclear architecture, and gene regulation in mammalian cells. *Nature Reviews Genetics*, 2, 292–301.

Cremer, T., Cremer, M., Dietzel, S., Müller, S., Solovei, I., & Fakan, S. (2006). Chromosome territories—a functional nuclear landscape. *Current Opinion in Cell Biology*, 18, 307–316.

Cremer, T., Cremer, M., Hübner, B., Strickfaden, H., Smeets, D., Popken, J., ... Cremer, C. (2015). The 4D nucleome: evidence for a dynamic nuclear landscape based on co-aligned active and inactive nuclear compartments. *FEBS Letters*, 589, 2931–2943. doi: 10.1016/j.febslet.2015.05.037

Damjanovic, A. K., Yang, Y., Glaser, R., Kiecolt-Glaser, J. K., Nguyen, H., Laskowski, B., ... Weng, N. P. (2007). Accelerated telomere erosion is associated with a declining immune function of caregivers of Alzheimer's disease patients. *The Journal of Immunology*, 179, 4249–4254.

Dubois, B., Feldman, H. H., Jacova, C., Dekosky, S. T., Barberger-Gateau, P., Cummings, J., ... Scheltens, P. (2007). Research criteria for the diagnosis of Alzheimer's disease: revising the NINCDS-ADRDA criteria. *The Lancet Neurology*, 6, 734–746.

Duin, R. P. W. (2007). *PRTools, a Matlab toolbox for pattern recognition*. Delf, Netherlands: Delft University of Technology.

Forero, D. A., González-Giraldo, Y., López-Quintero, C., Castro-Vega, L. J., Barreto, G. E., & Perry, G. (2016). Meta-analysis of telomere length in Alzheimer's disease. *Journals of Gerontology Series A: Biological Sciences and Medical Sciences*, 71, 1069–1073. doi: 10.1093/gerona/glw053

Folstein, M. F., Folstein, S. E., & McHugh, P. R. (1975). Mini-mental state. A practical method for grading the cognitive state of patients for the clinician. *Journal of Psychiatric Research*, 12, 189–198.

François, M., Fenech, M. F., Thomas, P., Hor, M., Rembach, A., Martins, R. N., ... Leifert, W. R. (2016). The Australian imaging biomarkers and lifestyle study research group. High content, multi-parameter analyses in buccal cells to identify Alzheimer's disease. *Current Alzheimer Research*, 13, 787–799.

Fritz, A. J., Barutcu, A. R., Martin-Buley, L., van Wijnen, A. J., Zaidi, S. K., Imbalzano, A. N., ... Stein, G. S. (2016). Chromosomes at work: organization of chromosome territories in the interphase nucleus. *Journal of Cellular Biochemistry*, 117, 9–19. doi: 10.1002/jcb.25280

Gadji, M., Vallente, R., Klewes, L., Righolt, C., Wark, L., Kongruttanachok, N., ... Mai, S. (2011). Nuclear remodeling as a mechanism for genomic instability in cancer. *Advances in Cancer Research*, 112, 77–126. doi: 10.1016/B978-0-12-387688-1.00004–1

Gauthier, S., Patterson, C., Chertkow, H., Gordon, M., Herrmann, N., Rockwood, K., ... Soucy, J. P. (2012). 4th Canadian consensus conference on the diagnosis and treatment of dementia. *Canadian Journal of Neurological Sciences*, 39, S1–S8.

Hebert, L. E., Weuve, J., Scherr, P. A., & Evans, D. A. (2013). Alzheimer disease in the United States (2010–2050) estimated using the 2010 census. *Neurology*, 80, 1778–1783.

Herrmann, N. & Gauthier, S. (2008). Diagnosis and treatment of dementia: 6. management of severe Alzheimer disease. *Canadian Medical Association Journal*, 179, 1279–1287.

Hu, Y. S., Cang, H., & Lillemeier, B. F. (2016). Super-resolution imaging reveals nanometer- and micrometer-scale spatial distributions of T-cell receptors in lymph nodes. *Proceedings of the National Academy of Sciences of the United States of America*, 113, 7201–72096. doi: 10.1073/pnas.1512331113

Ioannou, D., Kandukuri, L., Simpson, J. L., & Tempest, H. G. (2015). Chromosome territory repositioning induced by PHA-activation of lymphocytes: a 2D and 3D appraisal. *Molecular Cytogenetics*, 8, 47. doi: 10.1186/s13039-015-0146-3

Kirmes, I., Szczurek, A., Prakash, K., Charapitsa, I., Heiser, C., Musheev, M., ... Reid, G. (2015). A transient ischemic environment induces reversible compaction of chromatin. *Genome Biology*, 16, 246. doi: 10.1186/s13059-015-0802-2

Klein, H. U., Bennett, D. A., & De Jager, P. L. (2016). The epigenome in Alzheimer's disease: current state and approaches for a new path

to gene discovery and understanding disease mechanism. *Acta Neuropathologica*, 132, 503–514. doi: 10.1007/s00401-016-1612-7

Kuroda, M., Tanabe, H., Yoshida, K., Oikawa, K., Saito, A., Kiyuna, T., . . . Mukai, K. (2004). Alteration of chromosome positioning during adipocyte differentiation. *Journal of Cell Science*, 117, 5897–95903.

Lajoie, V., Lemieux, B., Sawan, B., Lichtensztejn, D., Lichtensztejn, Z., Wellinger, R., . . . Knecht, H. (2015). LMP1 mediates multinuclearity through downregulation of shelterin proteins and formation of telomeric aggregates. *Blood*, 125, 2101–2110. doi: 10.1182/blood-2014-08-594176

Lopez Perez, R., Best, G., Nicolay, N. H., Greubel, C., Rossberger, S., Reindl, J., . . . Huber, P. E. (2016). Super-resolution light microscopy shows nanostructure of carbon ion radiation-induced DNA double-strand break repair foci. *FASEB Journal*, 30, 2767–2776. doi: 10.1096/fj.201500106R

Louis, S. F., Vermolen, B. J., Garini, Y., Young, I. T., Guffei, A., Lichtensztejn, Z., . . . Mai, S. (2005). C-Myc induces chromosomal rearrangements through telomere and chromosome remodeling in the interphase nucleus. *Proceedings of the National Academy of Sciences of the United States of America*, 102, 9613–9618.

Luengo Hendriks, C. L., Rieger, B., van Ginkel, M., van Kempen, G. M. P., & van Vliet, L. J. (1999). *DIPimage: a scientific image processing toolbox for MATLAB*. Delf, Netherlands: Delft University of Technology.

Luengo Hendriks, C. L., van Kempen, G. M. P., & van Vliet, L. J. (2007). Improving the accuracy of isotropic granulometries. *Pattern Recognition Letters*, 28, 865–872.

Markaki, Y., Gunkel, M., Schermelleh, L., Beichmanis, S., Neumann, J., Heidemann, M., . . . Cremer, T. (2010). Functional nuclear organization of transcription and DNA replication: a topographical marriage between chromatin domains and the interchromatin compartment. *Cold Spring Harbor Symposia on Quantitaive Biology*, 75, 475–492. doi: 10.1101/sqb.2010.75.042

Matarazzo, M. R., Boyle, S., D'Esposito, M., & Bickmore, W. A. (2007). Chromosome territory reorganization in a human disease with altered DNA methylation. *Proceedings of the National Academy of Sciences of the United States of America*, 104, 16546–11651.

Mathur, S., Glogowska, A., McAvoy, E., Righolt, C., Rutherford, J., Willing, C., . . . Garcia, A. (2014). Three-dimensional quantitative imaging of telomeres in buccal cells identifies mild, moderate, and severe Alzheimer's disease patients. *Journal of Alzheimer's Disease*, 39, 35–48. doi: 10.3233/JAD-130866

McDowell, I., Kristjansson, B., Hill, G. B., & Hebert, R. (1997). Community screening for dementia: The Mini Mental State Exam (MMSE) and Modified Mini-Mental State Exam (3MS) compared. *Journal of Clinical Epidemiology*, 50, 377–383.

McKhann, G., Drachman, D., Folstein, M., Katzman, R., Price, D., & Stadlan, E. M. (1984). Clinical diagnosis of Alzheimer's disease: report of the NINCDS-ADRDA Work Group under the auspices of Department of Health and Human Services Task Force on Alzheimer's disease. *Neurology*, 34, 939–944.

Meaburn, K. J. (2016). Spatial Genome Organization and its emerging role as a potential diagnosis tool. *Frontiers in Genetics*, 7, 134. doi: 10.3389/fgene.2016.00134

Mehta, I. S., Amira, M., Harvey, A. J., & Bridger, J. M. (2010). Rapid chromosome territory relocation by nuclear motor activity in response to serum removal in primary human fibroblasts. *Genome Biology*, 11, R5. doi: 10.1186/gb-2010-11-1-r5

Nasreddine, Z. S., Phillips, N. A., Bedirian, V., Charbonneau, S., Whitehead, V., Collin, I., . . . Chertkow, H. (1995). The Montreal Cognitive Assessment, MoCA: a brief screening tool for mild cognitive impairment. *Journal of the American Geriatrics Society*, 53, 695–699.

O'Donovan, A., Tomiyama, A. J., Lin, J., Puterman, E., Adler, N. E., Kemeny, M., . . . Epel, E. S. (2012). Stress appraisals and cellular aging: a key role for anticipatory threat in the relationship between psychological stress and telomere length. *Brain, Behavior, and Immunity*, 24, 573–579. doi: 10.1016/j.bbi.2012.01.007

Ridler, T. W. & Calvard, S. (1978). Picture thresholding using an iterative selection method. *IEEE Transactions on Systems, Man, and Cybernetics*, 8, 630–632.

Righolt, C. H., Guffei, A., Knecht, H., Young, I. T., Stallinga, S., van Vliet, L. J., . . . Mai, S. (2014). Differences in nuclear DNA organization between lymphocytes, Hodgkin and Reed-Sternberg cells revealed by structured illumination microscopy. *Journal of Cellular Biochemistry*, 115, 1441–1448. doi: 10.1002/jcb.24800

Righolt, C. H., Knecht, H., & Mai, S. (2016). DNA superresolution structure of reed-sternberg cells differs between long-lasting remission versus relapsing Hodgkin's lymphoma patients. *Journal of Cellular Biochemistry*, 117, 1633–1637. doi: 10.1002/jcb.25456

Sathitruangsak, C., Righolt, C. H., Klewes, L., Tammur, P., Ilus, T., Tamm, A., . . . Mai, S. (2015). Quantitative superresolution microscopy reveals differences in nuclear DNA organization of multiple myeloma and monoclonal gammopathy of undetermined significance. *Journal of Cellular Biochemistry*, 116, 704–710. doi: 10.1002/jcb.25030

Schermelleh, L., Carlton, P. M., Haase, S., Shao, L., Winoto, L., Kner, P., . . . Sedat, J. W. (2008). Subdiffraction multicolor imaging of the nuclear periphery with 3D structured illumination microscopy. *Science*, 320, 1332–1336. doi: 10.1126/science.1156947

Sehgal, N., Fritz, A. J., Vecerova, J., Ding, H., Chen, Z., Stojkovic, B., . . . Berezney, R. (2016a). Large-scale probabilistic 3D organization of human chromosome territories. *Human Molecular Genetics*, 25, 419–436. doi: 10.1093/hmg/ddv479

Sehgal, N., Seifert, B., Ding, H., Chen, Z., Stojkovic, B., Bhattacharya, S., . . . Berezney, R. (2016b). Reorganization of the interchromosomal network during keratinocyte differentiation. *Chromosoma*, 125, 389–403. doi: 10.1007/s00412-015-0546-5

Solovei, I., Cavallo, A., Schermelleh, L., Jaunin, F., Scasselati, C., Cmarko, D., . . . Cremer, T. (2002). Spatial preservation of nuclear chromatin architecture during three-dimensional fluorescence in situ hybridization (3D-FISH). *Experimental Cell Research*, 276, 10–23.

Solovei, I., Kreysing, M., Lanctôt, C., Kösem, S., Peichl, L., Cremer, T., . . . Joffe, B. (2009). Nuclear architecture of rod photoreceptor cells adapts to vision in mammalian evolution. *Cell*, 137, 356–368. doi: 10.1016/j.cell.2009.01.052

Tanabe, H., Müller, S., Neusser, M., von Hase, J., Calcagno, E., Cremer, M., . . . Cremer, T. (2002) Evolutionary conservation of chromosome territory arrangements in cell nuclei from higher primates. *Proceedings of the National Academy of Sciences of the United States of America*, 99, 4424–4429.

Thomas, P., O'Callaghan, N. J., & Fenech, M. (2008). Telomere length in white blood cells, buccal cells and brain tissue and its variation with ageing and Alzheimer's disease. *Mechanisms of Aging and Development*, 129, 183–190. doi: 10.1016/j.mad.2007.12.004

Urban, M. A., Barclay, R. S., Sivaguru, M., & Punyasena, S. W. (2016). Cuticle and subsurface ornamentation of intact plant leaf epidermis under confocal and super-resolution microscopy. *Microscopy Research and Technique*, doi: 10.1002/jemt.22667. [Epub ahead of print].

Verbeek, P. W. & van Vliet, L. J. (1993). Estimators of 2D edge length and position, 3D surface area and position in sampled grey-valued images. *Bioimaging*, *1*, 47–61.

Vermolen, B. J., Garini, Y., Mai, S., Mougey, V., Fest, T., Chuang, T. C., . . . Young, I. T. (2005). Characterizing the three-dimensional organization of telomeres. *Cytometry A*, *67*, 144–150. *Erratum in: Cytometry A* (2007), 71, 345.

Wilczynski, G. M. (2014). Significance of higher-order chromatin architecture for neuronal function and dysfunction. *Neuropharmacology*, *80*, 28–33. doi: 10.1016/j.neuropharm.2014.01.016

Xie, W., Horn, H. F., & Wright, G. D. (2016). Super-resolution microscopy of the nuclear envelope and associated proteins. *Methods in Molecular Biology*, *1411*, 83–97. doi: 10.1007/978-1-4939-3530-7_4

## SUPPORTING INFORMATION

Additional Supporting Information may be found online in the supporting information tab for this article.